Journal of Electronic Research and Application

Research Article

Numerical Simulation on Air Swirl flow to Improve UV Disinfection Efficiency

Sinan Xu

Xi'an Gaoxin No.1 High School, 2AP1, China

Abstract: Affected by COVID-19, disinfection and purification in public space, such as ordinary school, had aroused wide public concern. This study presents an improved structure of nowadays medical used UV air purifier and discusses about its efficiency optimization, by utilizing following processes: Firstly, establishing the inner structure of the machine on computer and setting up the boundary conditions. Secondly, employing CFD (Computational Fluid Dynamics) to proceed the simulation of air swirl and the time used, and analyzing the relationship between different parameters and time. Finally, combining optimized parameters to obtain the best time used. The optimized structure efficaciously reduces the cost of machine, making utilization in the classroom become possible.

Key words: Fluid mechanics; Ultraviolet disinfection; Efficiency; Time delay; Numerical simulation

Publication date: September, 2020

Publication online: 30 September, 2020

****Corresponding author:*** Sinan Xu, sinan@163.com

1 Introduction

With the wide spread of COVID-19 pandemic, nowadays people are paying more attention on the epidemic prevention. In public spaces, such as classroom, opening windows to allow a good indoor air circulation is the best approach to block the spread of the virus. However, opened room would affect the working qualities of those indoor used devices, such as air conditioning system and ordinary air purifier. In the certain area holding no capability to install the ventilation system, a device with lower cost, which allows the human-machine coexistence and simultaneously working between air filtration and disinfection would efficaciously solve the problem[1].

Nowadays matured air sterilization technologies are plasma disinfection[2,3], photocatalysis disinfection [4], and UV-light air disinfection (ultraviolet rays with wavelength from 280nm to 200nm) [5]. The former two possess low efficiency when utilized in the public spaces with precondition in terms of large air flow, while the UVC technology can provide fast, highly efficient working process in the hospital or other populated areas. Ordinary ultraviolet circulating air sterilizer in medical use has carried this technology. Initially, airborne particulates are filtrated by HEPA (High Efficiency Particle Air Filter) or other cutting-edge filtration equipment. Then, the air flow inside the machine is irradiated by UVC light or LED ultraviolet array with no leaking radiation to proceed the sterilization. Finally, the air goes through a titanium dioxide photocatalyst filter[7] to make the second sterilization of air flow[8]. Nevertheless, there still exist disadvantages that the machine contains high power consumption of UV light, the extremely high cost, and the noisy of fans, which restrains its utilization in classrooms.

This study states that increasing the efficiency of disinfection on ultraviolet circulating air sterilizer can effectively solve the problem and makes it possible to employ the machine in the classroom. Under ideal conditions, in the limited space inside the machine, increasing the time of air flow to be irradiated by UV-light can enhance the amount of irradiation, boosting the effect of purification[9]. The technological reform based on this idea can lower the power consumption of UV-light (decrease the produce of ozone), reduce the number of circulation (decreasing air flux), and minimize the noisy. Thus, a technology which can effectively delay the time of air flow can enhance the

efficiency of sterilization. This study employs CFD (Computational Fluid Dynamics) to research the time spent of air flow inside the machine and the cost of the machine's structure, in order to utilize it in the classroom in school with air circulation standard of $450m^3/h$[10].

This study presents an improved structure of ordinary ultraviolet circulating air sterilizer. The machine contains two parts. The upper one is disinfection part, and the lower one is filtration part. Air flow enters from lower part and straightly go up to the outlet at top. This study designs a spiral blade installed around a centrifugal fan to make the air flow swirl up inside the device, and optimizes the structure by changing the parameters of blade to increase the time of air flow and lowering the power of ultraviolet light in the condition that the amount of irradiation is higher than 10 000μW.s/cm^2 to kill the virus. A photocatalyst filter and an active carbon filter layer are also installed at the outlet to make the secondary sterilization and avoid the ultraviolet light escaping to outside, as it is detrimental to students' health.

2 Physical model

The model is a cylinder with height 1.5 m and diameter 0.5 m and separated into upper disinfection part and lower filtration. This study focuses on the simulation of disinfection tank at the top. Figure 1 and Figure 2 display the three-dimensional model and the detailed structure diagram of the machine, respectively. As shown below, the tank is 800 mm height, 500 mm inner diameter, with ventilating duct at the bottom, installed with a centrifugal fan of 74 mm height and 224 mm external diameter. At the top of the fan is a disk with thickness of 10mm and diameter of 400mm downward connected with spiral blades. At the center of tank is an UVC-light (low pressure mercury lamp with vapor pressure from 1.3~13 pa (0.01~0.1 mmHg) emits ultraviolet ray with wavelength of 253.7 nm) with height 700 mm and diameter 70 mm. At the top is the outlet with a cover plate.

3 Theoretical analysis

The paper deduces theoretic derivations of the time of air flow to pass through the tank in the standard conditions with spiral blade installed by Bernoulli equation and continuity equation, as well as the time used by original machine without blades.

1）Theoretical analysis on the model with spiral

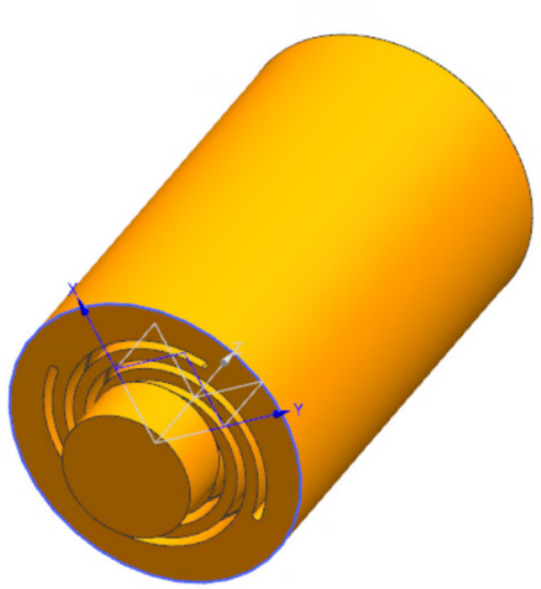

Figure 1. Fluid domain model of tank

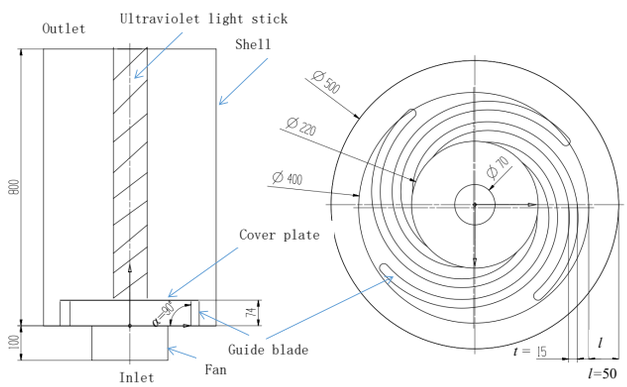

Figure 2. Configutation of tank

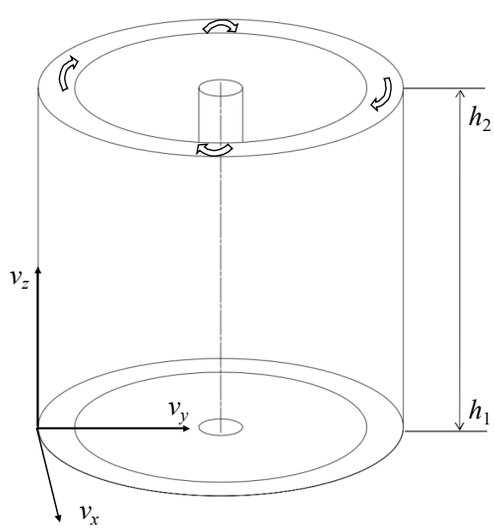

Figure 3. Theoretic model

blades

Bernoulli equation:

$p + 0.5\rho v^2 + pgh = C$

C is constant.

The velocity of spiral air can be separated by, v_x, v_y, v_z, which are defined by three different directions x, y, z. Since the air flow is basically moving along the inner wall, v_y can be ignored.

Calculating the average velocity of air flow moving from inlet to outlet.

According to Bernoulli equation and conditions of inlet and outlet:

$$\boldsymbol{p_1 + 0.5\rho v_{z1}^2 + \rho g h_1 = p_2 + 0.5\rho v_{z2}^2 + \rho g h_2}$$

The subscript "1" represents inlet, and subscript "2" represents outlet.

After transformation:

$$v_{z2}^2 - v_{z1}^2 = 2(p_1 - p_2)/\rho - 2\rho g(h_2 - h_1) \quad (1)$$

According to the performance of the fan, the entrance pressure is approximately 101013.5Pa, the exist pressure is 101000Pa. The density of the air is 1.29kg/m^3. The distance from h_1 to h_2 is the height of the tank, which is 0.8m. Thus:

$$v_{z2}^2 - v_{z1}^2 = 0.71 m^2/s^2$$

According to the conservation of mass:

$$v_{z1}A_1 = v_{z2}A^2 \quad (2)$$

A_1 is the area of the cover plate at the top of spiral blades (diameter 400mm), which is 0.0704m^2; A_2 is the plate area at the outlet of the machine (diameter 415mm), which is 0.0611m^2.

According to (1) and (2):

v_{z1} = 1.69m/s

v_{z2} = 1.47m/s

Given that the v_z is increasing linearly from inlet to outlet, the average velocity v_z=1.58m/s.

Therefore, the time of the air flow is:

$t = (h_2 - h_1)/v_z = 0.8/1.58 = 0.506s$

Total velocity is:

v = 450/3600/0.0704 = 1.77m/s

Thus, $v_x = (v_2 - v_{z2})0.5 = 0.798$m/s

The circumference of the air flow to make a circle is 3.14*0.5 = 1.57m

The time use of the air flow to finish one circle:

t_1 = 1.57/0.798 = 1.96s

Theoretical number of the circulation:

$n = t/t_1$ = 0.506/1.96 =0.23

2) Theoretical analysis on the original model without spiral blades

Time of the air flow without blades= $(h_2 - h_1)/v$=0.8/1.77=0.452s

According to the calculation, the spiral blades do delay the time of the air flow. Original time:0.452s, time of advanced structure with spiral blades: 0.506s, which is increased by 111.95% from original one.

4 Numerical simulation

4.1 Structural parameters

The article physically focuses on the study of spiral blades at the bottom of the tank, for the structure of blades holds more possibility to affect the time delay. In order to make the process of changing different variables become more convenient, the article defines the blades' shape as a helix which is spread from center to outside, and defines five parameters: number of blades, blades' length (total length of each curve), the angle with horizontal plane, blade thickness, and the smallest distance between blades and the tank inner wall. Utilizing control variable method, the article sets up standard value of these parameters, and then changes different variables to obtain the relationship between time delay and each parameter. Standard values: the number, a=4. The length of blades, d=597mm. Angle, θ=90°. Thickness, h=15mm. Distance between blades and inner wall, w=50mm.

4.2 Control equations

All of the flow will be controlled by conservation of mass, momentum, and energy. Three basic law of conservation:

Conservation of mass can be described as: The increase in the mass of the fluid micro-element in a unit time is equal to the net mass flowing into the micro-element in the same time interval, expressed in mathematical form as the following formula:

$$\frac{\partial \rho}{\partial t} + \frac{\partial(\rho u)}{\partial x} + \frac{\partial(\rho v)}{\partial y} + \frac{\partial(\rho w)}{\partial z} = 0 \quad (3)$$

Where t is the time ρ is density， u, v, w are the Euclidean vectors of velocity in the directions of x, y, z.

Conservation of momentum can be described as: The rate of change of the momentum of the fluid in the micro-element body with respect to time is equal to the sum of various external forces acting on the micro-element body, which is Newton's second law.

$$\frac{\partial(\rho u)}{\partial t}+\frac{\partial(\rho uu)}{\partial x}+\frac{\partial(\rho uv)}{\partial y}+\frac{\partial(\rho uw)}{\partial z}$$
$$=-\frac{\partial p}{\partial x}+\frac{\partial}{\partial x}\left(2\mu\frac{\partial u}{\partial x}+\lambda\nabla\bullet\mathbf{u}\right)+\frac{\partial}{\partial y}\left[\mu\left(\frac{\partial u}{\partial y}+\frac{\partial v}{\partial x}\right)\right]+\frac{\partial}{\partial z}\left[\mu\left(\frac{\partial u}{\partial z}+\frac{\partial w}{\partial x}\right)\right]+F_x \quad (4)$$

$$\frac{\partial(\rho v)}{\partial t}+\frac{\partial(\rho vu)}{\partial x}+\frac{\partial(\rho vv)}{\partial y}+\frac{\partial(\rho vw)}{\partial z}$$
$$=-\frac{\partial p}{\partial y}+\frac{\partial}{\partial x}\left[\mu\left(\frac{\partial u}{\partial y}+\frac{\partial v}{\partial x}\right)\right]+\frac{\partial}{\partial y}\left(2\mu\frac{\partial v}{\partial y}+\lambda\nabla\bullet\mathbf{u}\right)+\frac{\partial}{\partial z}\left[\mu\left(\frac{\partial v}{\partial z}+\frac{\partial w}{\partial y}\right)\right]+F_y \quad (5)$$

$$\frac{\partial(\rho w)}{\partial t}+\frac{\partial(\rho wu)}{\partial x}+\frac{\partial(\rho wv)}{\partial y}+\frac{\partial(\rho ww)}{\partial z}$$
$$=-\frac{\partial p}{\partial z}+\frac{\partial}{\partial x}\left[\mu\left(\frac{\partial u}{\partial z}+\frac{\partial w}{\partial x}\right)\right]+\frac{\partial}{\partial y}\left[\mu\left(\frac{\partial v}{\partial z}+\frac{\partial w}{\partial y}\right)\right]+\frac{\partial}{\partial z}\left(2\mu\frac{\partial w}{\partial z}+\lambda\nabla\bullet\mathbf{u}\right)+F_z \quad (6)$$

Where p is the pressure on the body of microelement, λ is second Viscosity（normally equals to -2/3）, μ is dynamic Viscosity, $\nabla * u$ is the divergence of the velocity, Fx、Fz、Fz are the forces on the body of microelement.

$$\nabla\bullet\mathbf{u}=\frac{\partial u}{\partial x}+\frac{\partial v}{\partial y}+\frac{\partial w}{\partial z} \quad (7)$$

The conservation of energy can be described as: The rate of increase of energy in the micro-element body is equal to the net heat flow into the micro-element body plus the work done by the physical and surface forces on the micro-element body, which is the first law of thermodynamics. Expressed in mathematical form:

$$\frac{\partial(\rho T)}{\partial t}+\frac{\partial(\rho uT)}{\partial x}+\frac{\partial(\rho vT)}{\partial y}+\frac{\partial(\rho wT)}{\partial z}$$
$$=\frac{\partial}{\partial x}\left(\frac{k}{c_p}\frac{\partial T}{\partial x}\right)+\frac{\partial}{\partial y}\left(\frac{k}{c_p}\frac{\partial T}{\partial y}\right)+\frac{\partial}{\partial z}\left(\frac{k}{c_p}\frac{\partial T}{\partial z}\right)+S_T \quad (8)$$

4.3 Mesh generation and boundary conditions

Since the spiral blades contain complexn structure, it is very hard to use structured mesh. This study employs ANSYS ICEM to proceed the unstructured mesh generation. Figure 4 is the mesh model of the machine, which only includes fluid domain. The model is mainly consisted of tetrahedral mesh. In order to make the calculation be more accurate, the area near the wall is meshed by prism grid. The first layer thickness is 0.01mm, mesh growth ratio is 1.2, the number of layers is 10. The largest mesh size is 3mm. This strategy obtains a total number of meshes to be 3 million, which can satisfy the accuracy and economy.

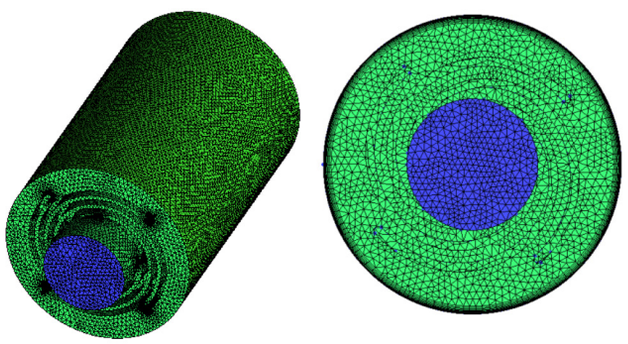

Figure 4. Mesh model

Figure 5 Presents the numerical model. The inlet is given by a certain velocity, which is 3.2m/s. The outlet pressure is set as 1 atmosphere, and the wall is adiabatic with no slip. The turbulence model of the calculation is k-epsilon model, which is the most common used one in engineering. The difference scheme adopts the second-order central difference and the PIMPLE algorithm. The calculation is transient, the time step is 0.01s, and the total time for solving the model is 6 s. The calculated convergence criterion is that the residuals of all terms are below 10^{-5} or the number of solving steps reaches more than 1000 steps.

5 Simulation results

This article makes a simulation targeted on five parameters (a, number of blades; d, length of blades; θ, the angle of blade with horizontal plane; h, thickness; w, distance between blades and inner wall). The relationship between different variables and time can be obtained by changing each single parameter.

Standard value of parameters: a=4, d=597mm, θ=90°, h=15mm, w=50mm.

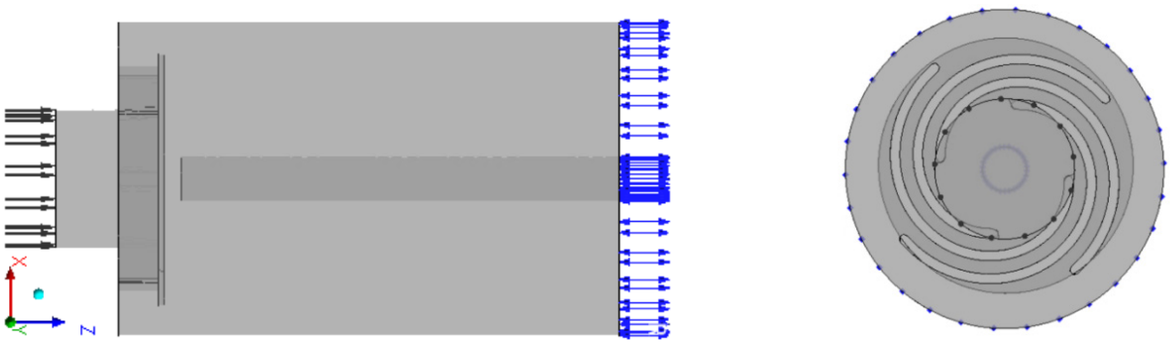

Figure 5. Numerical model

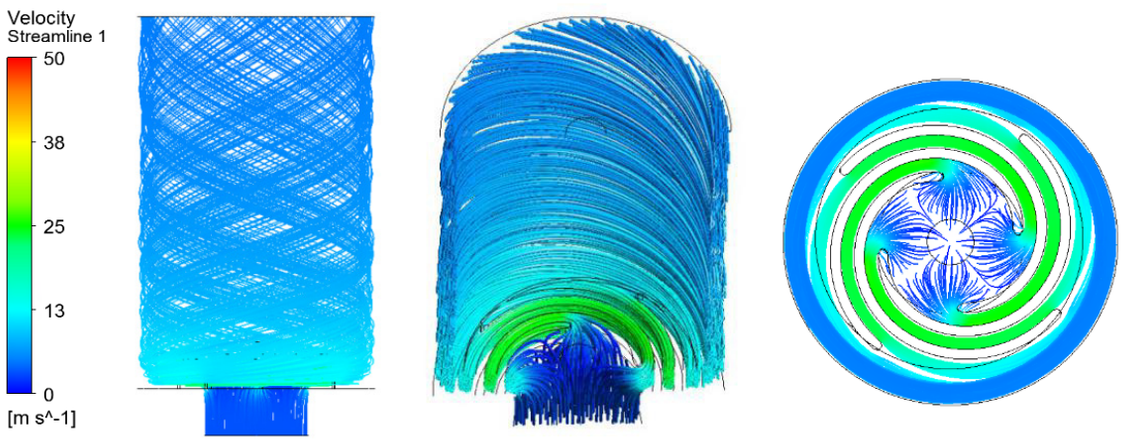

（a）lateral view （b）bird's-eye view （c）bottom view

Figure 6. Flow distribution of tank in basic parameters

Figure 6 displays the distribution of the flow field in the tank. It can be seen that the air inside the tank is swirling up in vortex, the velocity between the blades is the fastest, and then it becomes slower from the bottom to the top of the machine.

5.1 The effect of the number of blades

Standard value: a=4. The simulation is performed twice without changing other variables. The other values: a_1=2, and a_2=6. Figure 7 shows the relationship between time-delay and the number of blades by the analysis of three simulations, which is almost a linear relationship. The more the number of blades, the less the time delay would be.

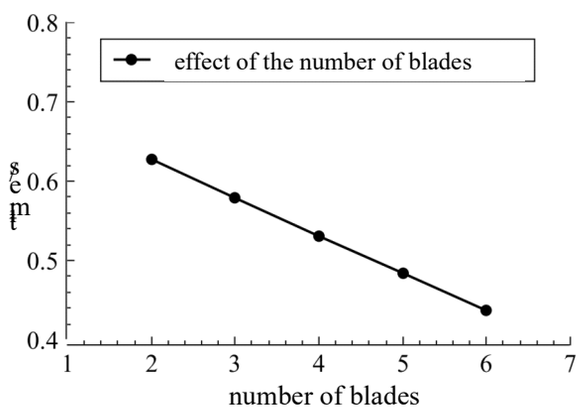

Figure 7. Relationship between time-delay and the number of blades

Figure 8 illustrates the flow distribution in three simulations, which could be used to analyse the reason why time-delay and the number of blades represents the relationship as showing above. With the increasing number of blades, the distance between each blades will decrease correspondingly, which increases the presure because of the reduced space, therefore increases the velocity of the air flow (initial velovity). In the graph, colors of flow lines represents the velocity. The slower air flows are represented by blue lines, and faster ones are red. It is apprent that the more amount of blades, the higher the velocity, which reduces the time used for air to pass through the tank. However, one single blade is not enough to make a swirl of air flow and will increase the time instead.

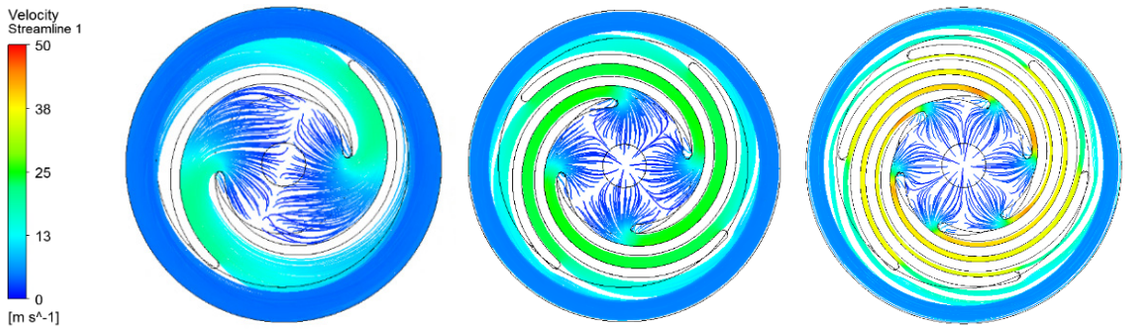

（a）a1=2　　（b）a=4　　（c）a2=6

Figure 8. Flow distribution of tank in different number of blades

5.2 The effect of length of blades

Standard value d=597mm. The others are d_1=376mm and d_2=857mm.

By analyzing the data, Figure 9 presents the relationship between the time dely and the length of blade, which also gives a linear relationship: the longer the blade, the less time there is.Figure 10 shows the distribution of flow field in the tank at three different variables. Because space is limited, increasing the length of blade can occupy certain area as the path for air flow, therefore increase the pressure and velocity at the bottom.

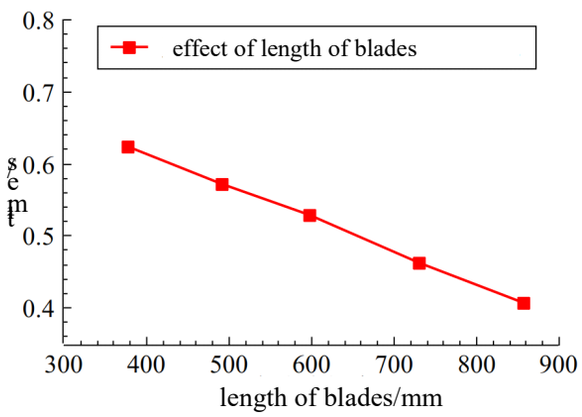

Figure 9. Relationship between time-delay and the length of blades

5.3 The effect of the blade angle

This study defines the angle of blades with horizontal plane ($>$ 90° when outward tilt, $<$ 90° when inward tilt). Standard value is θ=90°. The others are θ_1=60° and θ_2=120°. Figure 11. Plots the relationship between time delay and the angle of blades.

Figure 12 presents the distribution of tank in three different angles. According to the analysis, when the blade tilts to center, a cavity with a small inside and a wide outside is formed between the blades. When

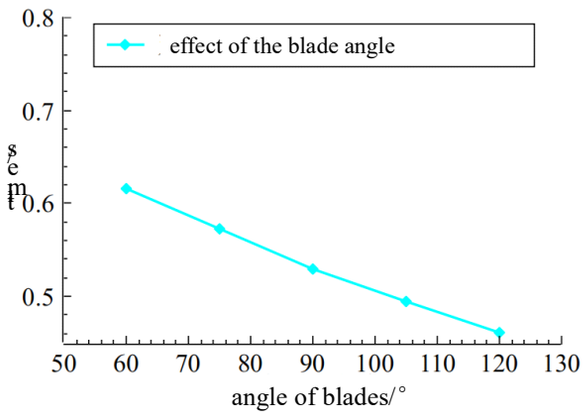

Figure 11. Relationship between time-delay and the angle of blades

the air just flows into the blades, because of the small space and high pressure, the air velocity is very high. As the air continue flowing, with the volume of the cavity between the blades increases, the air velocity will decrease because of the decreased pressure. On the graph, when the air go out from the blade, the color of velocity line is light blue which is more slower than the red one as the air just comes in, as shown in Figure 12 (a). When the blade tilts to the outside of the arc, a cavity with a wide inside and small outside is formed between the blades. Thus the air velocity increases gradually from the inside to the outside of the cavity. When the air flows out of the blade, the air velocity is red, as shown in Figure 12 (c), so the delay time is shortened.

5.4 The effect of the thickness of blades

Standard value h=15mm. The others are h_1=5mm and h_2=25mm.

Figure 13 presents the relationship between time and thickness, which is approximitely linearity. The thicker the blades, the less the delay time.

Figure 14 shows the flow field distribution of three

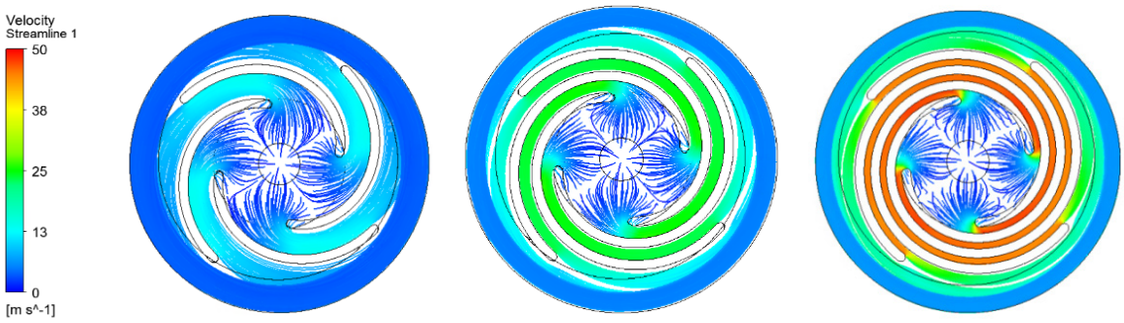

（a）d1=376mm　　（b）d=597mm　　（c）d2=857mm

Figure 10. Flow distribution of tank in different lengths of blades

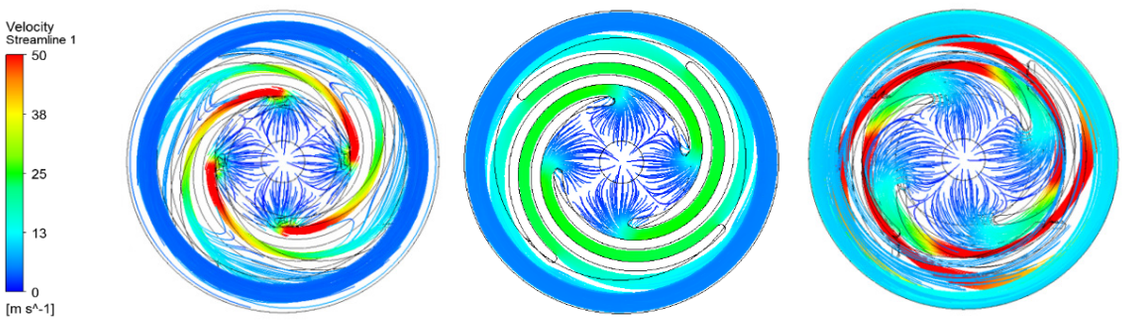

（a） θ 1=60°　　（b） θ =90°　　（c） θ 2=120°

Figure 12. Flow distribution of tank in different angles of blades

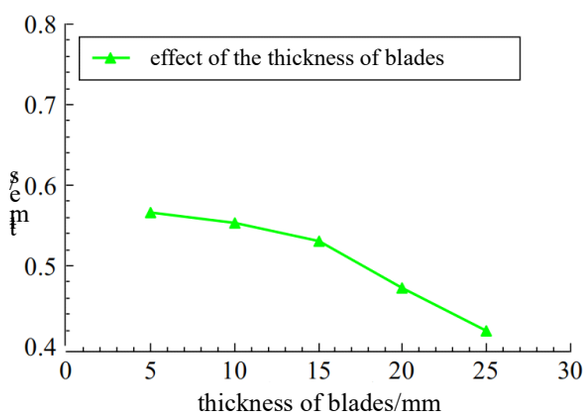

Figure 13 Relationship between time-delay and the thickness of blades

different conditions. According to the graph, thinner blades allow more space for the air flow, as the thickness of blades increases, the decreased space will also enhance pressure, then increases the velocity and shorted the time used.

5.5 The effect of the distance between blades and the inner wall

The distance is the minimum one between the outermost wall of the blades and the inner wall of the disinfection tank. The standard value is w=50. The others are w_1=25mm and w_2=75mm respectively.

Figure 15 presents the relationship between the distance and time, which is not linearity. The graph shows that w=35.5 is the rough maximum value. With w=35.5 as the center, the larger the distance, the shorter the delay time with faster declines. The smaller the distance, the delay time also decreases slightly.

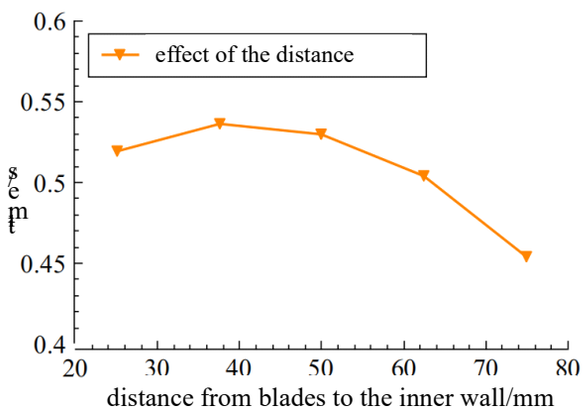

Figure 15 Relationship between time-delay and the distance from blades to the inner wall

Figure 16 plots the distribution of air flow in three different conditions. The air velocities in the three tanks should have a linear relationship that rises sequentially, instead of a parabolic-like relationship as shown in Figure 15. Since the air moves spirally close to the inner wall, when the distance between the blade and the inner wall of the tank is 25-50mm, the region of air movement is less affected by this distance, so the delay time is not significantly changed. When the distance is greater than 50mm, the spiral motion of the air close to the wall is weakened, and the vertical upward motion is strengthened. The distance between the blades is reduced to increase the velocity, therefore the delay time will be shortened.

5.6 Result of optimization

After obtaining the optimized parameters of the blade, the article presents a simulation of the tank with the

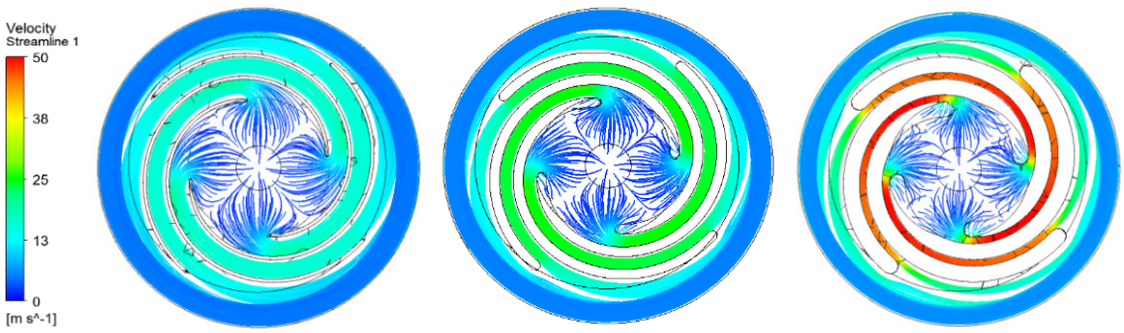

（a）h1=5mm （b）h=15mm （c）h2=25mm

Figure 14 Flow distribution of tank in different angles of blades

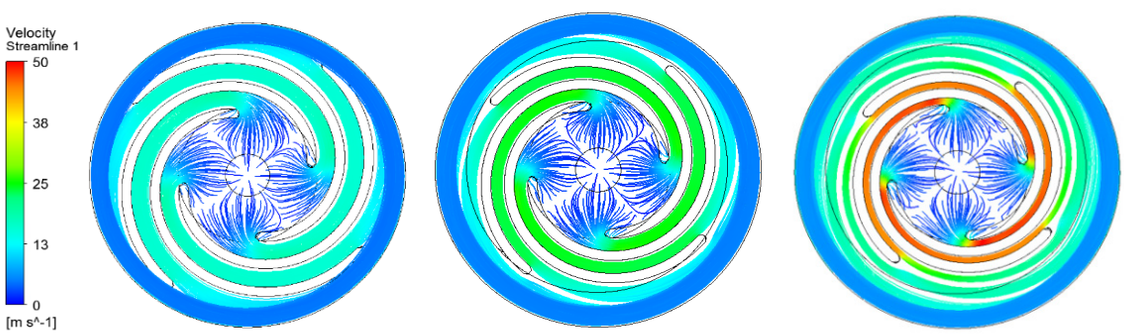

（a）w1=25mm （b）w=15mm （c）w2=75mm

Figure 16 Flow distribution of tank in different distances

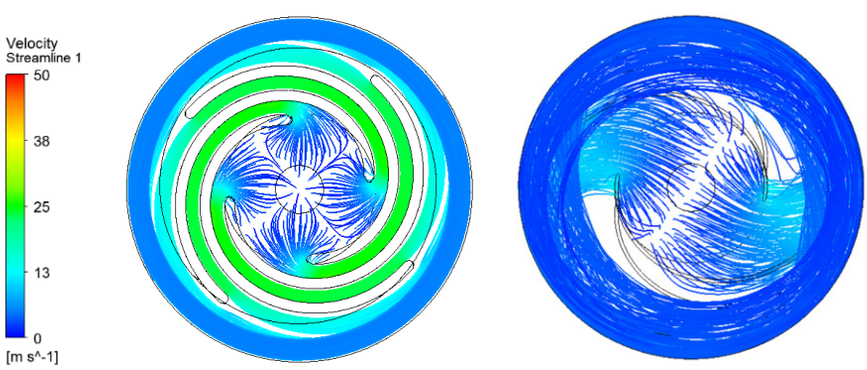

（a）w1=25mm （b）w=15mm （c）w2=75mm

Figure 17 Comparison between basic and improved structures

optimized structure and compares it with the original one. (Figure 17)

The air flow time of the machine with standard variables of the blade is 0.53s, and the optimized delay time is 1.171s, which is increased by 120.94%. The time of the air passing directly to the top of the original machine is 0.452s, which means the optimized structure increases the time by 158.85%.

6 Verification by practical experiment

In order to verify the accuracy of simulation, the article conducts the following experiment to measure the time used of air flow to pass through the tank.

6.1 Apparatus

Stainless steel barrel (inner diameter 500mm, height 800mm), parameter-optimized stainless steel blade (blade thickness 1.5mm, length 376mm, diameter 425mm, height 74mm), 220V vortex fan (air volume 450m^3/h) (see Figure 20 for the physical device) , MS6252A handheld anemometer, AS-K6 digital noise meter, digital multimeter, tape measure, paper knife, EVA sponge tape, electrical tape.

6.2 Procedure

1. Dig a hole in the center of the bottom of the stainless steel barrel (diameter 161mm).
2. Install the fan at the bottom of the blade module.
3. Install the blade module on the bottom of the stainless steel barrel.
4. Lead out the fan's power cord and make insulation protection, test the voltage.
5. Seal the air duct with EVA sponge tape at the air inlet.
6. Use a tape measure to mark the scale on the inner wall of the disinfection tank from bottom to top.
7. Place the tank in stable.
8. Three sets of experiments are carried out with a handheld anemometer, and each set of experiments tests the wind speed 7 times from bottom to top with an interval of 10 cm each time.

6.3 Experiment results

Table 1 lists the data collected.

Average velocity:

First experiment: v_1=（1.15+0.93+0.76+0.53+0.55+0.43+0.54）/7=0.70m/s

Second experiment: v_2=（1.15+0.93+0.79+0.56+0.55+0.43+0.56）/7=0.71m/s

Third experiment: v_3=（1.15+0.94+0.73+0.53+0.54+0.46+0.54）/7=0.70m/s

Air flow time:

First experiment: t_1= (h_2 - h_1)/v_1 =0.8/0.70=1.14s

First experiment: t_2= (h_2 - h_1)/v_2 =0.8/0.71=1.13s

Third experiment: t_3= (h_2 - h_1)/v_3 =0.8/0.70=1.14s

The three sets of experimental data are in good similarity with the simulated data (simulation time is 1.17s), which proves the accuracy of the numerical simulation.

Table 1. Experiment results

Distance from bottom（cm）	Experiment 1 (m/s)	Experiment 2 (m/s)	Experiment 3 (m/s)
10	1.15	1.15	1.15
20	0.93	0.93	0.94
30	0.76	0.79	0.73
40	0.53	0.56	0.53
50	0.55	0.55	0.54
60	0.43	0.43	0.46
70	0.54	0.56	0.54

Some problems are still found durcing the test: The noise of the machine is too loud, mainly caused by the resonance of the stainless steel blades during the diversion process; These experimental data are not measured accurately because of the limited equipment resources (time of air flow passing from air inlet to the outlet), leading to experimental errors. In order to apply this technology to public populated places such as school classrooms, improvements are still needed in terms of materials and engineering technology.

7 Conclusion

This paper mainly discusses the efficiency optimization problem of the improved UV ultraviolet air sterilizer by numerical simulation, which mainly refers to the problem of extending the flow time of air in the disinfection tank. The main conclusions are as follows:

(1) The smaller the number of blades (the number of blades≠1), the longer the delay time.

(2) The shorter the blades length, the longer the air flow time.

(3) The blade is deflected inward, increasing the delay time, and is deflected outward, reducing the delay time.

(4) The thinner the blades, the longer the delay time.

(5) The distance between the spiral blades and the tank's inner wall should be approximately 25mm-50mm. The shorter the distance, the longer the delay

（a）tank(stainless steel barrel)　（b）Bottom of the tank　（c）blade and fan module

Figure 20. Experimental device

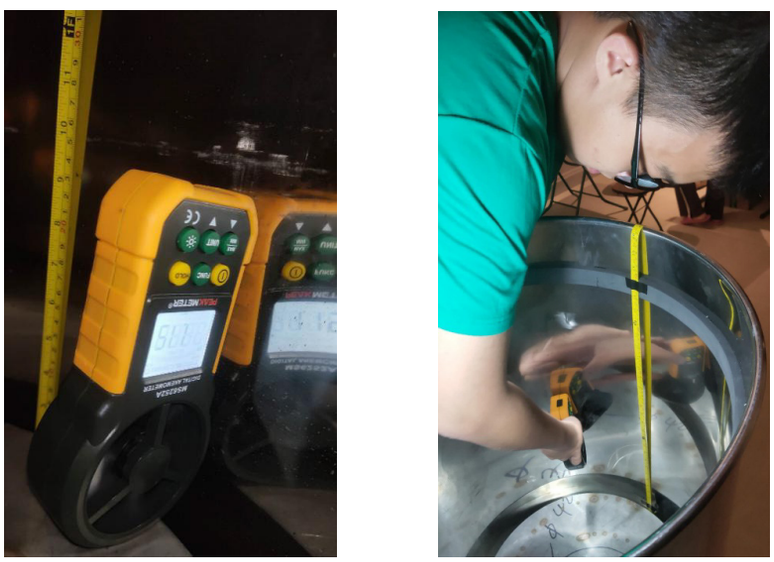

Figure 21 Experiment process

time.

(6) The optimized delay time is 1.171s, which increases 120.94% on delay time of the reference structure, and 158.85% on the original machine. According to conclusions above, it is feasible to use this method to increase the irradiation time of ultraviolet disinfection.

In terms of the technological innovation of the ultraviolet circulating air sterilizer, the application of this technology can effectively improve the antivirus efficiency and reduces the power consumption and cost of the product.

8 Acknowledgement

Here I sincerely thank Mr. Zhu Kaixuan, my physics teacher, for his careful guidance on this article. It was my first time to write a paper. Whether it is the analysis of the study content or structuring the hackling of the article, Mr. Zhu put forward many constructive suggestions for me and helped me a lot to solve the problem in the paper. It is fortunate to meet Dr. Xi Lei from Xi'an Jiaotong University. He is serious and careful and treats academic research very rigorously. He had helped me to overcome any difficulties, especially the simulation on the ANYSYS and theoretic analysis of the time passing through the machine.

References

[1] Yan Ping, Mumma S A. Study of the dedicated outdoor air system[J]. Heating ventilating & Conditioning, 2003, 33(6):44-49. c

[2] Zuyi Chen, Liwang Lin, Xiaona Li. Experimental study on the efficacy of the plasma air-sterilizing machine on air disinfection and purificationc[J]. Chinese Journal of Infection Control,

2007, 6(002):112-114.
[3] KITANO,Katsuhisa, IKAWA,Satoshi, TANI,Atsushi. Plasma Sterilization Technique for Disinfection Treatments and Its Physicochemical Model[J]. Chemical Engineering of Japan, 2011, 75.
[4] Yuwen Zhong, Yajing Wang, Huizhen Chen, et al. Study on indoor air purification and disinfection effect of a photocatalyst air purification disinfectior[J]. Chinese Journal of Disinfection, 2014, 31(011):1149-1151.
[5] Haiquan Jia, Xin Pan, Zongxing Zhang, etc. Efficacy of high intensity ultraviolet light air purifier on inactivation of bacterial aerosol[J]. Chinese Journal of Nosocomiology, 2011(10):2051-2053.
[6] Yufu Liu，The application of titanium dioxide photocatalyst to the metallic coating and metal protection technology Part IV-Performance evaluation and high capability of photocatalyst [J]. Electroplating & Finishing, 2006(09):41-43.
[7] Xinyu Huang, Shuang Xu, Xiaochun Jiang, Xinyu Li, Liqun Sun. Experimental observation on germicidal efficacy of circulating air ultraviolet air disinfector[J]. Chinese Journal of Disinfection,2004,21(2):141-142.
[8] GB 28235-2011 Safety and sanitary standard for ultraviolet appliance of air disinfection
[9] GB 50099-2011 Code for design of school.